

Anthropometry Data Measurement Methods of the Hand and Biomechanical Hand Model

Kyung-Sun Lee
Assistant Professor,
Department of Industrial Health,
Catholic University of Pusan, South Korea

Abstract:- The aim of this study was to suggest the measurement methods of anthropometric data for segment masses, centers of mass (COMs) of inertia segments, and gyration radii, which are required for the development of the biomechanical hand model. The segment masses were calculated based on the segment volumes using a density of 1.1 g/cm³. The COMs for the proximal and middle segments, and the distal segment were determined by approximating the phalanx with the cone frustum and a cylindrical homogeneous rigid body, respectively. Proximal and middle segment moments of inertia were determined by approximating the phalanx with the frustum of a conical homogenous rigid body. The biomechanical hand model consists of multiple complex structures, and 26 degrees of freedom were considered in total. The coordinate system for calculating the angle of each joint followed the recommendations of the International Society of Biomechanics. Euler angles were used to define the three-dimensional relative joint angular motion, and the Newtonian laws of statics were used to describe the forces and moments acting on the thumb and finger segments. This model can be used to perform kinetic and kinematic analysis for human hand posture.

Keywords: Anthropometric data; biomechanical hand model; kinematic; kinetic; hand posture

I. INTRODUCTION

The human hand has a high utility and more complicated mechanisms than many other body parts. The human hand consists of 27 small bones and 28 muscles. These bones and muscles are connected by 16 joints and have approximately 30 degrees of freedom. The bones of the hand consist of 14 phalanges, 5 metacarpal bones, and 8 carpal bones. These complex structures produce various postures such as flexion, extension, abduction, adduction, opposition, reposition, pronation, and supination. The complex mechanisms are generated by the large number of muscles and joints in the hand, and they enable various patterns of movement [1]. The human hand has a complex structure that enables various postures and movements in occupational and daily activities [2]. Many researchers have attempted to identify hand movements and postures using the biomechanical approach [3–6].

The physical load on the hand is typically evaluated using a biomechanical methodology. Biomechanics is the discipline that describes, analyzes, and assesses human movement based on physics, chemistry, mathematics, physiology, and anatomy principles [7]. Biomechanics concerns the mechanical behavior and component tissues of the musculoskeletal system when physical work is performed.

The application of biomechanics principles is important in the prevention of work-related musculoskeletal disorder to improve working conditions and performance. Biomechanical hand models are used in various fields such as ergonomics, industrial safety, product design, rehabilitation, robot design, and digital manufacturing. Anthropometric data for segment masses, moments of inertia, and radii of gyration are required for the development of biomechanical hand models.

Anthropometric data for segment masses, moments of inertia, and radii of gyration are required to develop biomechanical hand models. Buchholz and Armstrong [8] developed a kinematic model using ellipsoids to evaluate prehensile capabilities. The model was developed to simulate and predict hand prehensile posture to powerfully grasp objects such as ellipsoids or elliptical cylinders. Lee suggested a model to predict hand posture using optimization under the assumption that the hand configuration in a power prehension best conforms to the shape of the object [9]. These models explained how the grip posture varies in power grips, but they were insufficient for explaining other types of postures.

The aim of this study was to suggest measurement methods of anthropometric data for segment masses, centers of mass (COMs) of inertia segments, and radii of gyration, which are required for development of the biomechanical hand model and to develop a biomechanical model of the human hand.

II. HAND ANTHROPOMETRIC DATA

II.1 Segment masses

The segment masses were calculated based on the segment volume using a density of 1.1 g/cm³ [10]. The segment volume was estimated using the measured length between participants' distal and proximal joints (segment length) and the diameters of their knuckles. The volumes of the proximal and middle segments were approximated by that of the frustum of a cone, and the volume of the distal segment was approximated by that of a cylinder. The volumes of the proximal, middle, and distal segments were determined using equation 1 (proximal and middle segments) and 2 (distal segments) [11].

$$V = \pi H/3(R2 + Rr + r2) \quad (1)$$

$$V = \pi HR2 \quad (2)$$

III. BIOMECHANICAL HAND MODEL

where V is the volume of the segments, H is the segment length, R is the radius of the knuckle at the proximal joint, and r is the knuckle at the distal joint. Thus, the segment mass was calculated using the formula segment mass = density (1.1 g/cm^3) \times segment volume [12].

II. II Segment COMs

The COMs for the proximal and middle segments, and the distal segment were determined by approximating the phalanx with the frustum of a cone and a cylindrical homogeneous rigid body, respectively. The diameters of the knuckles were measured for each participant, and they are assumed to have a uniform density [12]. The COMs of the proximal and middle segments (equation 3) as well as distal segment (equation 4) can be determined by using the following equations.

$$COMs (Z) = H/4[R^2+2Rr+3Rr^2/R^2+Rr+r^2] \quad (3)$$

$$COMs (Z) = H/2 \quad (4)$$

Where H is the segment length, R is radius of the knuckle at the proximal joint, and r is the knuckle at the distal joint.

II. III Moments of inertia and radius of gyration

The moments of inertia of the proximal and middle segments were determined by approximating the phalanx with the frustum of a conical homogenous rigid body (equation 5) [13]. The knuckle diameters were measured for each participant.

$$I_z = 3m/10[R^5-r^5/R^3-r^3] \quad (5)$$

where I_z is the principle moment of inertia of a segment, m is the segment mass of each finger, R is the radius of the knuckles at the proximal joint, and r is the radius of the knuckles at the distal joint.

The moments of inertia of the distal segments were determined by approximating the phalanx with a cylindrical rigid body (equation 6).

$$I_x = 1/2 \cdot m \cdot R^2$$

$$I_y \text{ and } I_z = 1/12 \cdot m \cdot (3R^2 + H^2) \quad (6)$$

The radii of gyration, K_x , K_y , and K_z , of the segment about the x axis, y axis, and z axis, respectively, are defined as equation 7 [14].

$$K_x = \sqrt{I_x/m}, K_y = \sqrt{I_y/m}, K_z = \sqrt{I_z/m} \quad (7)$$

Where I_x , I_y , and I_z are the moments of inertia about the x axis, y axis, and z axis, respectively, and m is the segment mass.

III. I Kinematics skeleton

The biomechanical hand model consists of multiple complex structures. In total, 26 degrees of freedom were considered. For the thumb, the carpometacarpal, metacarpophalangeal (MCP), and interphalangeal joints were considered. The carpometacarpal joint of the thumb was modeled with three degrees of freedom: flexion/extension, abduction/adduction, and axial rotation. The MCP joint has flexion/extension and abduction/adduction, and the interphalangeal joint has flexion/extension [15]. For the four fingers (index, middle, ring, and little), the MCP, proximal interphalangeal (PIP), and distal interphalangeal (DIP) joints were considered. The MCP joints of these fingers were modeled with flexion/extension, abduction/adduction, and axial rotation. The PIP and DIP joints have only flexion/extension [16].

III. II Coordinate system

The coordinate system for calculating the angle of each joint followed the recommendations of the International Society of Biomechanics [17]. The positive direction of the X axis pointed forward, the positive direction of the Y axis pointed upward, and the positive direction of the Z axis pointed from the little finger to the thumb in the anatomical hand position. The flexion/extension angle of one marker per joint and two markers per segment was defined by the XY plane.

III. III Angular kinematic

Euler angles were used to define the three-dimensional relative joint angular motion. The angle of the finger joint was calculated using the Euler angle method to sequentially rotate Z , Y , and X . The first rotation about the Z axis is represented by F-E (θ), the second rotation about the Y axis is represented by Ab-Ad (ψ), and the third rotation about the X axis is represented by pronation/supination (ϕ) [15,18]. Two sets of unit vectors, I, J, K , and i, j, k , were fixed to the coordinate directions of X_p, Y_p, Z_p and X_d, Y_d, Z_d , respectively. Furthermore, the two coordinate systems on either side of the joint were transformed using the following matrix relationship [19]:

$$\begin{bmatrix} i \\ j \\ k \end{bmatrix} = \begin{bmatrix} c\phi c\theta & s\phi c\theta & -s\theta \\ -s\phi c\psi + c\phi s\psi & c\phi c\psi + s\phi s\psi & c\theta c\psi \\ s\phi c\psi + c\phi s\psi & -c\phi c\psi + s\phi s\psi & c\theta s\psi \end{bmatrix} \begin{bmatrix} I \\ J \\ K \end{bmatrix} \quad (8)$$

where c and s stand for the sine and cosine, respectively. The individual Euler angle can be determined from the following equation 9.

$$\begin{aligned} \theta &= \arcsin(-i \cdot K) \\ \phi &= A \tan 2(i \cdot J, i \cdot I) \\ \psi &= A \tan 2(j \cdot K, k \cdot K) \end{aligned} \quad (9)$$

where $\text{Atan2}(y, x)$ is the four-quadrant inverse tangent $\tan^{-1}(y/x)$ that results in the interval $[-\pi, \pi]$. The specific quartile is determined by the signs of x and y .

III. IV Joint reaction force and moment

The Newtonian laws of statics were used to describe the forces and moments acting on the thumb and finger segments. All thumb and finger segments were modeled as rigid bodies. The forces and moments for all fingers d were analyzed separately: $d = 1$ for the thumb, $d = 2$ for the index finger, $d = 3$ for the middle finger, $d = 4$ for the ring finger, and $d = 5$ for the little finger. The equilibrium equations for the forces are written for each segment i as follows in equation 10.

$$\sum F = f_{i-1,i}^d - f_{i,i+1}^d + m_i g = 0 \quad (10)$$

where the force $f_{i-1,i}^d$ is the force of the previous segment $i-1$ acting on segment i , and the negative force $f_{i,i+1}^d$ defines the action of segment $i+1$ on segment i . Additionally, m_i is the mass of the segment, and g is the gravitational acceleration.

The force $f_{i-1,i}^d$ is derived from the above equations. The negative force $f_{i,i+1}^d$ equals the external force f_e which is obtained through the pressure measurement (equation 11).

$$f_{3,4}^d = -f_e \quad (11)$$

The force vectors of the DIP joint ($i = 2$) are calculated based on the fingertip force (equation 12).

$$f_{2,3}^d = f_{3,4}^d - m_3^d g \quad (12)$$

The force vectors of the proximal interphalangeal (PIP) joint ($i = 1$) are calculated using as equation 13.

$$f_{1,2}^d = f_{2,3}^d - m_2^d \quad (13)$$

The force vectors of the MCP joint ($i = 0$) are calculated using as equation 14.

$$f_{0,1}^d = f_{1,2}^d - m_1^d g \quad (14)$$

The equilibrium equation for the moment is written for each segment i as follows (equation 15).

$$\sum M = M_{i-1,i}^d - M_{i,i+1}^d + r_i^L \times f_{i,i+1} = \dot{H}_i^o \quad (15)$$

where \dot{H}_i^o is the time derivative of the angular momentum at the origin of the i^{th} segment equation 16.

$$H_i^o = I_i^o \alpha_i + r_i^{\text{COM}} \times m_i g + \omega_i \times I_i^o \omega_i \quad (16)$$

where I_i^o is the inertia tensor of the link relative to the i^{th} segment, α_i is the angular acceleration of the segment, and r_i^L is the position of the $(i, i+1)^{\text{th}}$ segment relative to the $(i-1, i)^{\text{th}}$ segment. Further, r_i^{COM} is the position of the COM relative to the i segment, and ω_i is the angular velocity of the i^{th} segment. Figure 1 shows the free-body diagram for calculating joint forces and moments.

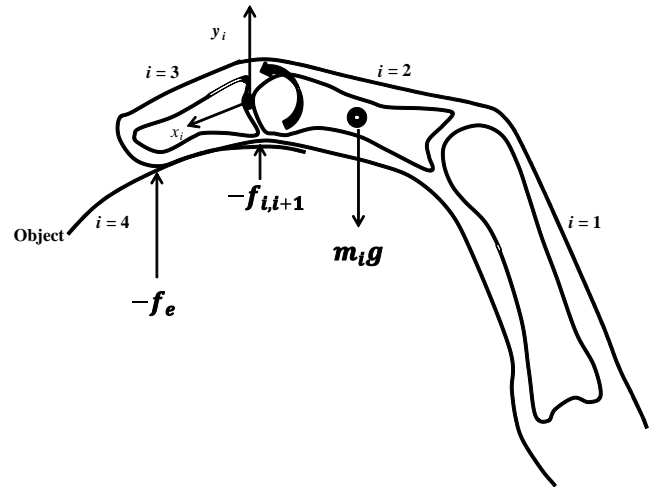


Fig. 1. Free-body diagram for calculating joint forces and moments.

IV. DISCUSSION

The human hand has a high utility and more complicated mechanisms than other body parts. Its complex mechanisms are generated by the large number of hand muscles and joints, and they enable various patterns of movement. These movements are used for purposes such as manipulating devices, picking up objects, pointing, climbing, playing musical instruments, drawing, and sculpting.

The high incidence and economic costs associated with cumulative trauma disorders of the hand have generated a significant amount of research on hand biomechanics. Thus, the ergonomics and occupational safety fields commonly use biomechanical hand models when conducting job analyses and task analyses, and designing hand tools and devices. Anthropometric data for segment masses, segment COMs, moments of inertia, and gyration radii are required for the development of biomechanical hand models. Thus, the objective of this study was to provide methods for the collection of anthropometric data. These anthropometric data were then used to calculate assumptions and physics and mathematics equations.

The biomechanical analysis of human hand movements can be divided into kinematics, kinetic, anthropometry, and electromyography. Kinetics is described as the internal and external forces that cause the movement. To perform kinematic and kinetic analyses, anthropometric factors including the anatomy and mechanics of the human hand must be considered. Euler angles are a common method used to explain the orientations of body segments including those of the hand in kinematics [20]. Most biomechanical finger models are based on the Landsmeer tendon pulley

model [21,22] in ergonomics that identifies finger movements in various hand postures and predicts the finger muscle and tendon forces in two-dimensional static conditions. In this study, a biomechanical model was developed to estimate the physical load according to hand posture.

V. CONCLUSION

The aim of this study was to suggest measurement methods of hand anthropometric data and to develop a hand biomechanical model that can describe hand postures during various grip and grasp movements. Biomechanical hand models can be used with kinematic and kinetic models to predict various hand postures. This information is required to design tools, controls, handles, and other objects that are grasped or otherwise used by the hand. The proposed hand biomechanical model can be applied for solving issues related to ergonomics, healthcare, and rehabilitation in industries.

ACKNOWLEDGEMENT

This study was supported by Basic Science Research Program through the National Research Foundation of Korea (NRF) funded by the Ministry of Education (NRF-2019R111A3A01061509).

REFERENCES

- [1] Smith RJ. Balance and kinetics of the finger under normal and pathological conditions. *Clinical Orthopaedics & Related Research*. 1974;104(1):92–111.
- [2] Domalain M, Vigouroux L, Danion F, Sevrez V, Berton E. Effect of object width on precision grip force and finger posture. *Ergonomics*. 2008;51(9):1441–1453.
- [3] Harding DC, Brandt KD, and Hillberry BM. Finger joint force minimization in pianists using optimization techniques. *Journal of Biomechanics*. 1993;26(12):1403–1412.
- [4] Butz KD, Merrell G, Nauman EA. A biomechanical analysis of finger joint forces and stresses developed during common daily activities. *Computer Methods in Biomechanics and Biomedical Engineering*. 2012;15(2):131–140.
- [5] Fok KS, Chou SM. Development of a finger biomechanical model and its considerations. *Journal of Biomechanics*. 2010;43(4):701–713.
- [6] An KN, Chao EY, Cooney WP, Linscheid RL. Forces in the normal and abnormal hand. *Journal of Orthopaedic Research*. 1985;3(2):202–211.
- [7] Winter DA. *Biomechanics and motor control of human movement*, (4th edition), John Wiley & Sons, New Jersey, 2005.
- [8] Buchholz B, Armstrong TJ. A kinematic model of the human hand to evaluate its prehensile capabilities. *Journal of Biomechanics*. 1992;25(2):149-162.
- [9] Lee SW, Zhang X. Development and evaluation of an optimization-based model for power-grip posture prediction. *Journal of Biomechanics*. 2005;38(8):1591-1597.
- [10] Esteki A, Mansour JM. A dynamic model of the hand with application in functional neuromuscular stimulation. *Annals of Biomedical Engineering*. 1997;25(3):440–451.
- [11] Stewart J. *Calculus: Early Transcendentals* (fifth edition). Thomson Learning, Inc. 2008.
- [12] Dempster WT. *Space Requirements of the Seated Operator*, WADC-TR-55-159. Aerospace Medical Research Laboratories. Wright-Patterson Air Force Base, OH. 1955.
- [13] Myers JA. *Handbook of Equations for Mass and Area Properties of Various Geometrical Shapes*, U. S. Naval Ordnance Test Station. 1962.
- [14] Pytel A, Kiusalaas J, *Engineering Mechanics: Dynamics* (second edition), Book/Cole Publishing Company. 1999.
- [15] Li ZM, Tang J. Coordination of thumb joints during opposition. *Journal of Biomechanics*. 2007;40(3):502-510.
- [16] Jenkins DB. *Hollinshead's Functional Anatomy of the Limbs and Back* (ninth edition). Elsevier. 2008.
- [17] Wu G, Van der Helm FCT, Veeger HEJ, Makhssous M, Van Roy P, Anglin C, et al. ISB recommendation on definitions of joint coordinate systems of various joints for the reporting of human joint motion-Part II: Shoulder, elbow, wrist and hand. *Journal of Biomechanics*. 2005; 38(5):981-992.
- [18] Su FC, Chou YL, Yang CS, Lin GT, An KN. Movement of finger joints induced by synergistic wrist motion. *Clinical Biomechanics*. 2005;20(5):491-497.
- [19] Chao EYS, An KN, Cooney WP, Linscheid RL, *Biomechanics of the Hand, A Basic Research Study*, World Scientific Publishing Co. Pte. Ltd., 1989.
- [20] Small CF, Bryant JT, Pichora DR. Rationalization of kinematic descriptors for three-dimensional hand and finger motion. *Journal of Biomedical Engineering*. 1992;14(2):133-141.
- [21] Spoor CW, Landsmeer JMF. Analysis of the zigzag movement of the human finger under influence of the extensor digitorum tendon and the deep flexor tendon. *Journal of Biomechanics*. 1976;9(9):561-566.

Acknowledgements: This study was supported by Basic Science Research Program through the National Research Foundation of Korea (NRF) funded by the Ministry of Education (NRF-2019R111A3A01061509).